The solution structure of the disulphide-linked homodimer of the human trefoil protein TFF1

Mark A. Williams[a,c], Bruce R. Westley[b], Felicity E.B. May[b], James Feeney[a,*]

[a] Molecular Structure Division, National Institute for Medical Research, Mill Hill, London NW7 1AA, UK
[b] Department of Pathology, Royal Victoria Infirmary, University of Newcastle, Newcastle upon Tyne NE1 4LP, UK
[c] Department of Biochemistry and Molecular Biology, University College London, Gower Street, London WC1E 6BT, UK

Received 20 November 2000; revised 30 January 2001; accepted 30 January 2001

First published online 13 March 2001

Edited by Thomas L. James

Abstract The trefoil factor family protein, TFF1, forms a homodimer, via a disulphide linkage, that has greater activity in wound healing assays than the monomer. Having previously determined a high-resolution solution structure of a monomeric analogue of TFF1, we now investigate the structure of the homodimer formed by the native sequence. The two putative receptor/ligand recognition domains are found to be well separated, at opposite ends of a flexible linker. This contrasts sharply with the known fixed and compact arrangement of the two trefoil domains of the closely related TFF2, and has significant implications for the mechanism of action and functional specificity of the TFF of proteins.

Key words: Trefoil factor family; TFF1; TFF1 dimer; Nuclear magnetic resonance; Solution structure

1. Introduction

The trefoil factor family (TFF) proteins are secreted proteins produced in large quantities in epithelial mucosa and appear to have an important role in maintenance of mucosal integrity of the gastrointestinal tract. Members of the family comprise one or more trefoil domains [1]. The trefoil motif consists of ~40 amino acids with several well-conserved features including six cysteine residues with essentially conserved spacings. Three closely related human TFF proteins are known. Human TFF1, previously known as pS2 or pNR-2, is a small, secreted protein of 60 amino acid residues and contains a single trefoil domain [2–5]. TFF3, previously designated intestinal trefoil factor, consists of 59 residues and also contains a single trefoil domain [6,7]. TFF2, previously called spasmolytic polypeptide, contains two trefoil domains in a single chain of 106 amino acids [8].

The physiological effects of the human trefoil proteins have been extensively investigated and reviewed [9,10] in recent years. These proteins are found in many cancers, including those of the breast and pancreas. This discovery, together with the finding that gastric tumours increase in mice lacking TFF1 [11], has stimulated much research in cancer-related areas [12]. However, presently much more is known about the role of trefoil proteins in normal tissue, where it seems highly likely that they have an important active role in wound healing in the mucosal epithelia of the gut. All three human trefoil proteins promote cell motility in cultured cells [13–15]. In TFF1, homodimerisation can take place via the formation of an intermolecular disulphide bond between the Cys^{58} residues of the two monomers [16]. Dimers of TFF1 and TFF3 have been identified in several tissues [16–18]. Furthermore, it has been shown that dimerisation of TFF1 plays a key role in both its motogenic and protective/healing effects [15]. It is plausible therefore that the biologically potent forms of all three of the human trefoil proteins contain two trefoil domains. The molecular mechanisms of the trefoil proteins protective and motogenic effects are not understood and may involve several distinct processes. The three trefoil proteins show distinct patterns of expression in normal and diseased tissue suggesting that each has distinct functions and possibly separate receptors. The proteins may be involved in the processing of mucin glycoproteins or formation of mucous structures [6,18]. It has been suggested that as the active forms of the molecule are dimeric the trefoil proteins may cross-link the mucin glycoproteins thereby stabilising the mucous layer [19]. Their role in promoting movement in wounded cells may involve recognition by specific receptors and the effects of TFF1 dimerisation suggest that the receptors may be involved in a bivalent interaction with surface residues from two trefoil domains.

Three-dimensional (3D) structures have been determined for three trefoil domains, one from human TFF1 [20] and two from porcine TFF2 [19,21,22]. The structures show that the cysteines pair in a 1–5, 2–4, 3–6 manner, forming a structure comprising three closely packed loops, with the third loop sandwiched between the first and second. A short α-helix is packed against two anti-parallel β-strands (Fig. 1). The conserved surface residues are localised in a small area on adjacent parts of the second and third loops, strongly suggesting that this area is a receptor/ligand binding site [19–21].

The N- and C-termini of porcine TFF2 are linked by a seventh disulphide bond, which helps to fix the relative orientation of its two trefoil domains. This produces a compact structure with the two domains in direct contact and the putative binding sites of each domain separated by 44 Å (dis-

E-mail: m.williams@biochemistry.ucl.ac.uk
E-mail: f.e.b.may@newcastle.ac.uk
*Corresponding author. Fax: (44)-20-8906 4477.
E-mail: jfeeney@nimr.mrc.ac.uk

Abbreviations: HSQC, heteronuclear single quantum correlation spectroscopy; NMR, nuclear magnetic resonance; NOE, nuclear Overhauser enhancement; NOESY, nuclear Overhauser enhancement spectroscopy

0014-5793/01/$20.00
PII: S0014-5793(01)02276-1

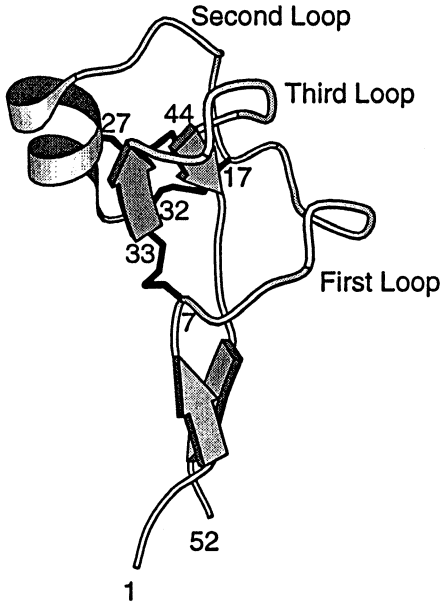

Fig. 1. A representation of the structure of TFF1 (residues 1–52 only) together with the complete native sequence (produced using MOLSCRIPT [30]). The cysteine side chains involved in the three characteristic disulphide linkages are numbered and shown in black. The putative binding site is centred on residues 19, 20 and 41–43 at the tops of the second and third loops.

tance between the Cα atoms of Pro22 and Pro71) and facing away from each other. Both TFF1 and TFF3 have a seventh cysteine residue close to the C-terminus (Cys^{58} in TFF1), capable of forming intermolecular disulphide bonds [16,17]. In our earlier study of TFF1 dimerisation was deliberately prevented by introducing a Ser^{58} mutation [23]. The resulting monomeric protein provided excellent spectra that allowed us to make essentially complete resonance assignments and to determine a high-resolution 3D solution structure [20,24]. We now report the structure of the dimeric form of the native protein.

2. Materials and methods

2.1. Protein expression and purification

The detailed protocols for the production and purification of the recombinant proteins have been described previously [16,20,23]. Briefly, the unlabelled proteins were purified from the periplasm of *Escherichia coli* HB101 cells transfected with pEZZ18:TFF1 Cys^{58} or TFF1 Ser^{58}. The fusion protein was purified by IgG–Sepharose affinity chromatography, cleaved with Factor X_a and the trefoil protein separated by a second passage through the IgG–Sepharose column. TFF1 Ser^{58} was purified further on a 1 ml Mono Q anion exchange. TFF1 Cys^{58} was first incubated with 50 mM cysteine then purified on Mono Q, and then the dimer was separated from the residual monomer by gel filtration on Superdex 75 (Pharmacia). The preparation of the ^{15}N-labelled TFF1 proteins differed only in being grown in *E. coli* JM109 (monomer) and BL21 cells (dimer) in modified M9 medium containing $(^{15}NH_4)_2SO_4$ as the sole nitrogen source.

2.2. Nuclear magnetic resonance (NMR) measurements

NMR experiments were performed on Varian Unity spectrometers operating at 500 and 600 MHz using the same pulse sequences as previously detailed for the monomer [20,24]. The previously reported ^{15}N-edited heteronuclear single quantum correlation spectroscopy (HSQC), $^{15}N^1H$-nuclear Overhauser enhancement spectroscopy (NOESY)–HSQC, $^1H^1H$-NOESY experiments on the TFF1 Ser^{58} monomer carried out at 298 K and $^1H^1H$-ROESY at 283 K in D_2O using 1 mM monomer in 4.5 mM potassium phosphate at pH* 5.9 (pH* refers to pH metre readings uncorrected for deuterium isotope effects) have been reprocessed and compared directly with the equivalent spectra from TFF1 dimer.

In the case of the unlabelled dimer, $^1H^1H$-total correlation spectroscopy and $^1H^1H$-NOESY experiments were first recorded using ~1.3 mM dimer at 298 K and pH* 5.9 in 90% H_2O/10% D_2O with 4.5 mM potassium phosphate. The sample was then lyophilised and redissolved in 100% D_2O. A series of 1D ^1H spectra and 2D $^1H^1H$-NOESY spectra were recorded at 298 K in the following 18 h in order to monitor the degree of protection of any slowly exchanging amide groups. Subsequently a $^1H^1H$-ROESY experiment was performed on this sample at 283 K. The sample was then lyophilised and redissolved in 90% H_2O/10% D_2O; 1D proton spectra were then also recorded at protein concentrations of ~1.3 mM and 130 μM. A 2D $^1H^1H$-NOESY spectrum was recorded following the addition of 4 mM Ca^{2+} (as $CaCl_2$) to the 1.3 mM dimer sample. 1D proton spectra were also recorded using ~0.5 mM dimer at pH* 5.8, 6.9 and 7.6 in the presence of 2 mM Ca^{2+}. The sample of uniformly ^{15}N-labelled protein was also used to measure the heteronuclear $^{15}N\{^1H\}$ steady state nuclear Overhauser enhancement (NOE) signals and to record 2D ^{15}N-edited HSQC and 3D $^{15}N^1H$-NOESY–HSQC spectra.

2.3. Spectrum analysis

The NMR spectra were processed using nmrPipe [25], and visualised and quantitated using ANSIG v3.3 [26] and XEASY [27]. The ^1H and ^{15}N shifts were referenced as described previously [20]. Mild resolution enhancement was obtained by applying a $\pi/2$ to $\pi/2.5$ shifted sine-squared apodisation function in all dimensions. Zero-filling was employed in all indirectly detected dimensions. Linear prediction was used to extend the data by one half in the heteronuclear dimension of 3D spectra. The final sizes of the data matrices were 8192×1024 real points for 2D homonuclear spectra, 4096×512 for 2D heteronuclear spectra and $1024\times512\times128$ for 3D spectra.

2.4. Structure calculations

The structural models for both the monomer and dimer were calculated using CNS 1.0 [28] with identical simulated annealing protocols (2000 steps/15 fs at 50 000 K, then 5000 cooling steps/5 fs of torsion dynamics, then 5000 steps/5 fs of cartesian dynamics cooling from 1000 K, then 200 steps of minimisation). The structure calculations began from an extended chain using different velocities for each repetition of the simulated annealing protocol. The protocol was repeated until 10 structures that satisfied the experimental restraints had been found.

3. Results

3.1. Assignment and experimentally derived restraints

The earlier assignment of the spectra of the TFF1 Ser^{58} mutant has been described in detail [20,24]. We have now made 35 additional NOE assignments for the monomer, resolving some earlier ambiguities. The sequential assignments of the dimer were made via direct comparison of peaks in the monomer and dimer NOESY and ROESY spectra, in conjunction with the observed NOE connectivities in the dimer spectra. In the ^{15}N-edited HSQC spectra of the dimer each pair of corresponding amino acids is represented by a single amide peak implying that the homodimer is symmetric in its time averaged form on the NMR timescale (ms). Consequently, NOESY peaks in the dimer spectra would not necessarily be assignable as specifically intra- or inter-chain, however as we already have spectra of the monomeric protein we have assumed that peaks occurring with the same chemical shifts (^1H within 0.03 ppm and ^{15}N within 0.3 ppm) in both monomer and dimer spectra are intra-chain. Remaining ambiguities were largely resolved by using ambiguous NOEs in several rounds of structure calculations, with explicit assign-

ments being made as the structural data supported them. The sequential assignments for the TFF1 Ser[58] monomer and the TFF1 dimer have been deposited at BioMagResBank.

The restraints used here for the structure calculations of the monomer are as described in detail previously [20], except for the changes to some distance restraints resulting from the new NOE assignments. The dimer restraints are identical to those of the Ser[58] monomer for residues 1–51, except for the addition of 13 distance restraints corresponding to very weak intra-chain NOEs, which are discernible in the dimer spectra because of the trefoil domain's effectively higher concentration. The angular and distance restraints for the C-terminal tail region 52–60 are substantially different from those of the monomer. In particular, there are 27 distance restraints for this tail region that are persistently ambiguous as to intra- and inter-chain assignment. In order to assess the impact of the sparse and ambiguous nature of the restraints for this region on the final structures, three sets of structures were calculated in which these restraints were (i) omitted, (ii) included and (iii) augmented by the addition of backbone torsion restraints designed to restrict residues 52–60 to allowed regions of the Ramachandran plot. As the structures generated were very similar for all three sets of restraints, we henceforth only consider the results of set (iii), which have been deposited, together with the structures generated from them, as entries r1hi7mr and 1hi7, respectively in the EBI Protein Data Bank and are summarised in Table 1.

3.2. The dimer's trefoil domains are intact, well separated and do not have a fixed orientation

The structures derived for both monomer (Ser[58] analogue) and dimer have well-defined trefoil domains (Fig. 2). The structures for the trefoil domains (residues 7–48) are essentially identical to that previously reported for TFF1 Ser[58] [20]. Also the β-sheet formed by part of the N- and C-termini (residues 3–6 and 49–51) is retained and, because of some of the spectral ambiguities that have now been resolved, is in fact somewhat better defined in these new monomer and dimer structures than in that previously reported [20]. Given the sparse and ambiguous nature of inter-chain NOEs, there is

Fig. 2. A view of the final family of 10 dimer structures, created by superimposing the residues from only one subunit at the centre of the figure. This shows that whereas an individual subunit is well defined by the experimental data, the dimer can adopt many conformations leading to a considerable variety of spacing and orientation of the putative binding sites.

Table 1
NMR restraints and structural statistics

		Monomer	Dimer
Restraints used in final structure calculation:			
Unambiguous NOEs:	long range ($\|i-j\|>4$)	171	356
	medium range ($1<\|i-j\|<4$)	111	226
	sequential ($\|i-j\|=1$)	217	434
	intra-residue	124	292
	total	623	1308
Ambiguous NOEs:	intra-chain	35	72
	intra-/inter-chain	–	27
Dihedral angles:	φ	43	48
	ψ	49	43
	χ	42	38
Hydrogen bonds		8	16
Disulphide bonds		3	7
Restraint violations per structure in the final ensembles of 10 structures[a]:			
Number of NOE constraint violations >0.2 Å		0 (0)	0 (0)
Number of dihedral angle violations $>2°$		0 (0)	0 (0)
XPLOR energies (kcal mol^{-1})[b]	E_{NOE}	0.5 ± 1.0 (2.6)	1.0 ± 1.0 (2.8)
	E_{CDIH}	0.1 ± 0.2 (0.6)	0.2 ± 0.3 (1.0)
	E_{TOTAL}	19 ± 10 (43)	40 ± 9 (62)
Structural statistics for the final ensembles:			
% of residues in the most favoured region of Ramachandran[c]		76	66[d]
Backbone pairwise rmsd of the trefoil domain (residues 7–47)		0.59	0.64
Heavy atom pairwise rmsd of the trefoil domain		1.42	1.38
Distance between trefoil domains (Pro20 Cα to Pro20 Cα)[a]		–	59 ± 12(72)

[a]Mean ± standard deviation (maximum value).
[b]The force constants used to calculate E_{NOE} were 50 kcal mol^{-1} Å^{-2} for 'normal' NOE constraints and 200 kcal mol^{-1} Å^{-2} for those representing hydrogen bonds. The force constant used to calculate E_{CDIH} was 200 kcal mol^{-1} rad^{-2}. E_{TOTAL} was calculated using the topallhdg5.1 and parallhdg5.1 parameters with PROLSQ non-bonded interactions [31]. Some torsion angle parameters were modified to more closely reflect the preferences observed in high-resolution crystal structures [32].
[c]Data from Procheck [33].
[d]The lower number of residues in the most favoured region is a consequence of strain in the C-terminal tail introduced by the restraints that are ambiguous as to inter- or intra-chain.

no strong restraint on the relative position of the two trefoil domains, which consequently adopt a variety of relative orientations in the calculated structures (Fig. 2). In all the calculated structures, even in the set calculated with no restraints on residues 52–60, the trefoil domains do not come into contact. Implying that the overall structure is rather constrained by the steric/packing properties of the peptide sequence near the disulphide junction itself. The adjacent prolines kink the chain and are relatively conformationally restricted and the disulphide bond itself forces the C-termini to cross each other at nearly 90° at Cys^{58}. Consequently, in the majority of structures the putative binding sites are facing almost directly away from each other with a separation of up to >50 Å (Pro20 Cα to Pro20 Cα distance), however a few face each other and consequently can have binding site separations as short as 36 Å.

The results of the structure calculations are supported by evidence from the comparison of chemical shifts and H/D exchange behaviour of the monomer and dimer. Changes of chemical shift of ^{15}N and ^{1}H backbone resonances provide an extremely sensitive indicator of the presence of new interactions in any complex on a residue-by-residue basis. Potentially significant changes in backbone or side chain chemical shifts are limited to residues 48–50 and the inevitable shifts around the new disulphide linkage, residues 56–60. This again implies no new interactions made by the trefoil domain. In the case of the β-sheet residues 48–50, there is no evidence to indicate a substantive change in structure, in particular the NOEs found for these residues, including 15 between N- and C-terminal tails, are identical in both monomer and dimer except for the greater line width of the dimer. However this region is known to be somewhat flexible [20] and we conclude that the shifts are due to changes in populations of similar structures in fast exchange. The reality of the non-interaction of the trefoil domains is also supported by the absence of differences in H/D exchange protection between monomer and dimer. This indicates that no new hydrogen bonds are formed nor are backbone accessibilities significantly altered upon formation of the dimer. Additional support for the non-association of the trefoil domains is found in our earlier observations of the complete lack of dimerisation of the Ser^{58} TFF1 in NMR [24] and analytic ultracentrifugation [16] experiments.

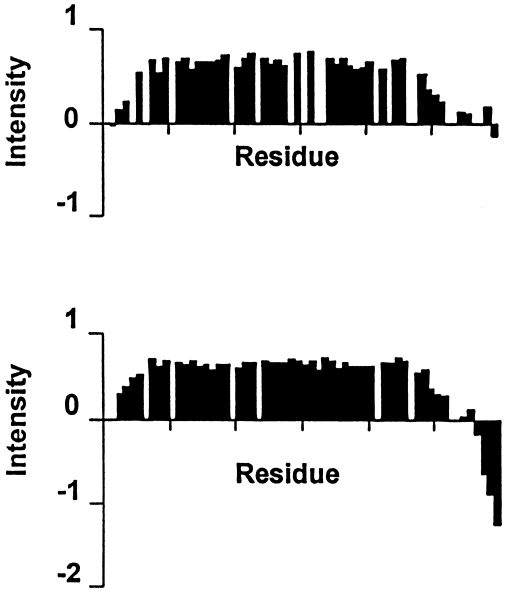

Fig. 3. The measured $^{15}N\{^{1}H\}$NOE values for the amide backbone groups of the native sequence dimer (top) and Ser^{58} monomer (bottom). Values below 0.5 over several successive residues indicate rapid local conformational change of the backbone on the ns timescale. The N- and C-terminal tails of the dimer exhibit much of the rapid motion seen in the monomer despite the presence of the disulphide cross-link. This suggests that the dimer structures in Fig. 2 are rapidly interconverting when the dimer is free in solution. The NOE values were measured at 14.1 T (600 MHz for ^{1}H), zero values are given for the prolines and for residues with peaks that cannot be accurately quantitated due to spectral overlap, of which there are more in the spectrum of the dimer due to its greater linewidths.

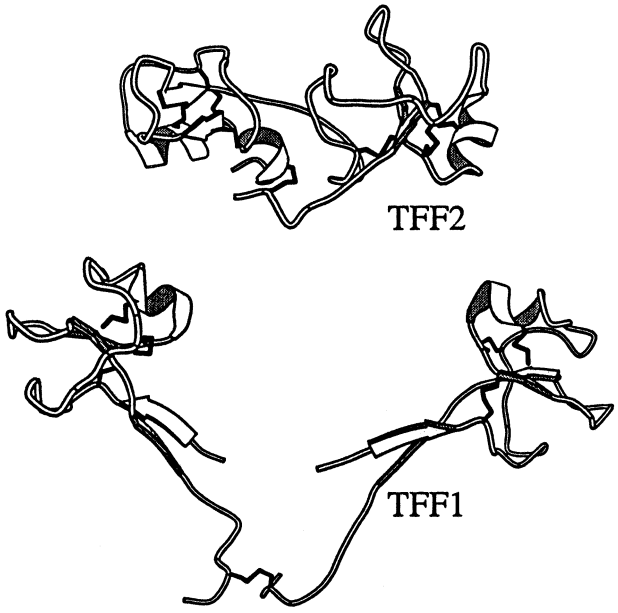

Fig. 4. A MOLSCRIPT [30] representation of the structures of TFF2 and the TFF1 dimer, illustrating the different separation and orientation of their trefoil domains. The secondary structure is represented only in the trefoil domain and the Cys side chains (disulphide bonds) are shown in black.

Data on the backbone dynamics of the dimer confirms the presence of a flexible linker region in the dimer. The heteronuclear NOE data for both monomer and dimer are shown in Fig. 3, residues 55–60 have particularly low values, which are characteristic of a high degree of flexibility. In the monomer the free C-terminal end is very flexible indeed with negative heteronuclear NOE values, although the C-terminal residues are less flexible in the dimer because of the disulphide bond formation, they still retain high mobility relative to the rest of the structure.

3.3. The local structure is unaffected by changes in protein concentration, pH or Ca^{2+} ions

There are eight glutamate residues surrounding the Cys^{58}–Cys^{58} disulphide bond in the TFF1 dimer. Several glutamates in close proximity can sometimes form binding sites for divalent metal ions and may have also have perturbed pK_a values. We considered the possibility that the conformation of the dimer might be modulated by changes in solution conditions. In particular, it is tempting to speculate that these residues in the TFF1 dimer may form a metal binding site, which may be involved in the function or regulation of TFF1. In view of the high calcium levels in some mucous granules [29] and the

possible role of trefoils in cross-linking mucins, this idea is particularly intriguing. However, we have found no evidence for local conformational change induced by the presence of calcium. Similarly there is no discernible effect on local structure between pH 5.6 and 7.6 (the range within which we can prepare useful NMR samples). Neither is there any evidence for changes in the oligomerisation of the protein with Ca^{2+}, pH or protein concentration (between 100 μM and 1 mM).

4. Discussion

It had been previously suggested that the structures of the TFF1 and TFF3 dimers could be very similar to the compact structure of TFF2. Homology models of the dimers were built on that basis in which the N- and C-terminal tail regions of the polypeptide chain fold in such a way as to interact with both of the trefoil domains, acting as the 'glue' sticking the domains together [17]. The present work provides no evidence for this kind of extensive interaction between the N- and C-terminal tails and the trefoil domains of TFF1 dimer.

We have found that the two trefoil domains of the TFF1 dimer, which contain the putative receptor/ligand recognition sites, do not adopt a fixed orientation with respect to one another, but are held apart on opposite ends of a flexible linker (Fig. 4). This observation has significant implications for the possible mechanism of action of the TFF of proteins. In any form of bidentate binding of the trefoil proteins, such as might occur in their suggested role as glycoprotein cross-linkers or for recognition of putative (dimeric?) receptors, the relative separation and orientation of the binding sites on the trefoil domains would obviously be important. Certainly, the members of the trefoil family would have different reach in any cross-linking role, for example, the closely spaced fixed distance binding sites of TFF2 (44 Å) could be specific for achieving a particular interaction and the variable distance (36–73 Å) and orientation of the TFF1 binding sites could offer greater versatility at the expense of some specificity. Such flexibility might be needed if TFF1 is acting as an adapter molecule binding to receptor binding sites on two different proteins and bringing them together. The TFF3 dimer, which has a shorter C-terminal tail, perhaps provides a reach intermediate between those of the other two trefoil proteins. Thus, it seems probable that differences in function/receptor specificity of the members of the human TFF are not only modulated by variations in amino acid composition of the putative recognition interface [20], but also by the substantially different orientation and separation of the two recognition sites in the biologically active forms of the molecules.

Acknowledgements: NMR experiments were performed at the MRC Biomedical NMR Centre in London. M.A.W. is grateful to the UK Medical Research Council for the award of a Research Fellowship.

References

[1] Thim, L. (1989) FEBS Lett. 250, 85–90.
[2] Masiakowski, P., Breathnach, R., Bloch, J., Gannon, F., Krust, A. and Chambon, P. (1982) Nucleic Acids Res. 24, 7895–7903.
[3] Prud'homme, J.F., Fridlansky, F., Le Cunff, M., Atger, M., Mercier-Bodard, C., Pichon, M.F. and Milgrom, E. (1985) DNA 4, 11–21.
[4] May, F.E.B. and Westley, B.R. (1986) Cancer Res. 46, 6034–6040.
[5] May, F.E.B. and Westley, B.R. (1988) J. Biol. Chem. 263, 12901–12908.
[6] Podolsky, D.K., Lynch-Devaney, K., Stow, J.L., Oates, P., Murgue, B., DeBeaumont, M., Sands, B.E. and Mahida, Y.R. (1993) J. Biol. Chem. 268, 6694–6702.
[7] Hauser, F., Poulsom, R., Chinery, R., Rogers, L.A., Hanby, A.M., Wright, N.A. and Hoffmann, W. (1993) Proc. Natl. Acad. Sci. USA 90, 6961–6965.
[8] Tomasetto, C., Rio, M.-C., Gautier, C., Wolf, C., Hareuveni, M., Chambon, P. and Lathe, R. (1990) EMBO J. 9, 407–414.
[9] May, F.E.B. and Westley, B.R. (1997) J. Pathol. 183, 4–7.
[10] Wright, N.A., Hoffmann, W., Otto, W.R., Rio, M.C. and Thim, L. (1997) FEBS Lett. 408, 121–123.
[11] Lefebvre, O., Chenard, M.-P., Masson, R., Linares, J., Dierich, A., LeMeur, M., Wendling, C., Tomasetto, C., Chambon, P. and Rio, M.-C. (1996) Science 274, 259–262.
[12] May, F.E.B. and Westley, B.R. (1997) J. Pathol. 182, 404–413.
[13] Dignass, A., Lynch-Devaney, K., Kindon, H., Thim, L. and Podolsky, D.K. (1994) J. Clin. Invest. 94, 376–383.
[14] Playford, R.J., Marchbank, T., Chinery, R., Evison, R., Pignatelli, M., Boulton, R.A., Thim, L. and Hanby, A.M. (1995) Gastroenterology 108, 108–116.
[15] Marchbank, T., Westley, B.R., May, F.E.B., Calnan, D.P. and Playford, R.J. (1998) J. Pathol. 185, 153–158.
[16] Chadwick, M.P., Westley, B.R. and May, F.E.B. (1997) Biochem. J. 327, 117–123.
[17] Chinery, R., Bates, P.A., De, A. and Freemont, P.S. (1995) FEBS Lett. 357, 50–54.
[18] Newton, J.L., Allen, A., Westley, B.R. and May, F.E.B. (2000) Gut 46, 312–320.
[19] Gajhede, M., Petersen, T.N., Henriksen, A., Petersen, J.F.W., Dauter, Z., Wilson, K.S. and Thim, L. (1993) Structure 1, 253–262.
[20] Polshakov, V.I., Williams, M.A., Gargaro, A.R., Frenkiel, T.A., Westley, B.R., Chadwick, M.P., May, F.E.B. and Feeney, J. (1997) J. Mol. Biol. 267, 418–432.
[21] De, A., Brown, D.G., Gorman, M.A., Carr, M.D. and Sanderson, M.R. (1994) Proc. Natl. Acad. Sci. USA 91, 1084–1088.
[22] Carr, M.D., Bauer, C.J., Gradwell, M.J. and Feeney, J. (1994) Proc. Natl. Acad. Sci. USA 91, 2206–2210.
[23] Chadwick, M.P., May, F.E.B. and Westley, B.R. (1995) Biochem. J. 308, 1001–1007.
[24] Polshakov, V.I., Frenkiel, T.A., Westley, B., Chadwick, M., May, F., Carr, M.D. and Feeney, J. (1995) Eur. J. Biochem. 233, 847–855.
[25] Delaglio, F., Grzesiek, S., Vuister, G.W., Zhu, G., Pfeifer, J. and Bax, A. (1995) J. Biomol. NMR 6, 277–293.
[26] Kraulis, P.J. (1989) J. Magn. Reson. 24, 627–633.
[27] Bartels, C., Xia, T-H., Billeter, M., Güntert, P. and Wüthrich, K. (1995) J. Biomol. NMR 5, 1–10.
[28] Brünger, A.T., Adams, P.D., Clore, G.M., DeLano, W.L., Gros, P., Grose-Kunstleve, R.W., Jiang, J.-S., Kuszewski, J., Nilges, M., Pannu, N.S., Read, R.J., Rice, L.M., Simonson, T. and Warren, G.L. (1998) Acta Cryst. D54, 905–921.
[29] Nyugen, T., Chin, W.C. and Verdugo, P. (1998) Nature 395, 908–912.
[30] Kraulis, P.J. (1991) J. Appl. Cryst. 24, 946–950.
[31] Linge, J.P. and Nilges, M. (1999) J. Biomol. NMR 13, 51–59.
[32] Laskowski, R.A., MacArthur, M.W., Moss, D.S. and Thornton, J.M. (1993) J. Appl. Cryst. 26, 283–291.
[33] Laskowski, R.A., Rullmann, J.A.C., MacArthur, M.W., Kaptein, R. and Thornton, J.M. (1996) J. Biomol. NMR 8, 477–486.